

PECULIAR FEATURES OF THE VELOCITY FIELD OF OB ASSOCIATIONS AND THE SPIRAL STRUCTURE OF THE GALAXY

A.M.Mel'nik

Sternberg Astronomical Institute, Moscow, Russia

anna@sai.msu.ru

Astronomy Letters, 2003, Vol. 29, pp. 304-310

Abstract

Some of the peculiar features of the periodic velocity-field structure for OB associations can be explained by using the Roberts-Hausman model, in which the behavior of a system of dense clouds is considered in a perturbed potential. The absence of statistically significant variations in the azimuthal velocity across the Carina arm, probably, results from its sharp increase behind the shock front, which is easily blurred by distance errors. The existence of a shock wave in the spiral arms and, at the same time, the virtually free motion of OB associations in epicycles can be reconciled in the model of particle clouds with a mean free path of 0.2–2 kpc. The velocity field of OB associations exhibits two appreciable nonrandom deviations from an ideal spiral pattern: a 0.5-kpc displacement of the Cygnus- and Carina-arm fragments from one another and a weakening of the Perseus arm in quadrant III. However, the identified fragments of the Carina, Cygnus, and Perseus arms do not belong to any of the known types of spurs.

Key words: kinematics and dynamics, Milky Way Galaxy, spiral pattern, OB associations.

Introduction

Here, we analyze some of the peculiar features or defects of the periodic velocity-field structure of OB associations (Mel'nik et al. 2001). First, we found no statistically significant variations in the azimuthal residual velocity across the Carina arm, although clearly see its variations across the Cygnus and Perseus arms. Second, OB associations exhibit the features of both collisional and collisionless motion. Third, the displacement of individual arm fragments from one another such that they do not form a single smooth spiral arm and the gaps in the spiral pattern should be explained.

Some of the peculiar features listed above can be explained by using the model of Roberts and Hausman (1984), in which the behavior of a system of dense clouds is considered in a perturbed potential. There is ample theoretical and observational evidence for the existence of small, unaccounted molecular gas condensations, from which giant molecular complexes are formed at certain times (Solomon et al. 1985; Pringle et al. 2001).

The response of a subsystem of elementary particle clouds to the propagation of a density wave over the stellar disk was first considered by Levinson and Roberts (1981). They assumed that clouds could collide inelastically with each other and coalesce in some cases. In contrast to a continuous gaseous medium, which responds to a potential perturbation by an abrupt jump of the density and velocity, a subsystem of dense particle clouds exhibits smoother variations in gasdynamical parameters across spiral arms (Levinson and Roberts 1981).

Roberts and Hausman (1984) considered the behavior of a subsystem of clouds with a velocity dispersion of $\Delta u = 6 \text{ km s}^{-1}$ and showed that the local frequency of cloud-cloud collisions increases sharply in spiral arms due to the crowding of cloud orbits in arms. This increase inevitably gives rise to a shock wave even in systems with a large cloud mean free path (see case G , $p = 2 \text{ kpc}$ in the above paper).

The study of molecular clouds in the Galaxy is complicated by the fact that, in general, we do not know their distances and observe their distribution in the (l, V_{LSR}) plane. However, the spiral structure of the Galaxy is difficult to analyze in the (l, V_{LSR}) plane and virtually impossible in the inner regions (Kwan and Veides 1987; Adler and Roberts 1992). Constructing and analyzing the velocity field of young stars, which, on average, have the same velocities as their parent molecular clouds, give a unique opportunity for studying the velocity field of molecular clouds and the Galactic spiral structure.

Analysis of the Velocity Field of OB Associations

The Periodic Velocity-Field Structure of OB Associations

Analysis of the velocity field of OB associations within 3 kpc of the Sun revealed periodic variations in the radial component V_R of residual velocity along the Galactic radius vector with a scale length of $\lambda = 2 \pm 0.2$ kpc and amplitude $f_R = 7 \pm 2$ km s⁻¹ (Mel'nik et al. 2001). Figure 1a shows the distribution of radial residual velocities V_R of OB associations along Galactocentric distance. The filled and open circles represent the associations located in the regions $0 < l < 180^\circ$ and $180 < l < 360^\circ$, respectively. This was done in order to separate the initial parts of the arms in quadrants I and II from their extensions in quadrants III and IV. The periodic variations of the two velocity components were assumed to be in the shape of sine waves. The parameters of the sine waves were determined by solving the equations for the line-of-sight velocities and proper-motions of OB associations in two regions: $30 < l < 180^\circ$ and $180 < l < 360^\circ$ (for more details, see Mel'nik et al. 2001). The minima in the radial residual velocity distribution determine the kinematical locations of the arm fragments, which we call the Carina (open circles, $R = 6.5$ kpc), Cygnus (filled circles, $R = 6.8$ kpc), and Perseus (filled circles, $R = 8.2$ kpc) arms.

In Fig. 1a we see no second minimum in the radial velocity distribution in the region $180 < l < 360^\circ$ (open circles). This second minimum should have corresponded to the extension of the Perseus arm in quadrant III. The local decrease in V_R is observed at a Galactocentric distance of $R = 8.5$ kpc, but it does not reach negative values.

As regards the azimuthal velocity field, periodic variations in the azimuthal component V_θ of residual velocity with an amplitude of $f_\theta = 7 \pm 2$ km s⁻¹ are observed in the region $30 < l < 180^\circ$ where the Cygnus and Perseus arms are located (Fig. 1b). The positions of the minima in the distributions of the radial (Fig. 1a) and azimuthal (Fig. 1b) residual velocities, which determine the kinematic locations of the Cygnus and Perseus arms, coincide, within the error limits. At the same time, no significant variations in the azimuthal residual velocity were found in the region $180 < l < 360^\circ$, where the Carina arm lies and where the imaginary extension of the Perseus arm could be located.

The interarm distance of $\lambda = 2$ kpc yields a mean arm pitch angle of $i = 5^\circ$ for the two-armed model of the spiral pattern. The Galactocentric distance of the Sun was assumed to be $R_0 = 7.1$ kpc (Rastorguev et al. 1994; Dambis et al. 1995; Glushkova et al. 1998).

The Profiles of Cloud-Velocities Variations in a Shock Wave

The coincidence of the positions of the minima in the radial and azimuthal velocity distributions in the Cygnus and Perseus arms suggests the existence of a shock wave and cloud-cloud collisions. In a shock wave, extremely negative values of the perturbations of the two velocity components must be reached at the same phase at the shock front (Roberts 1969; Roberts and Hausman 1984), while for a collisionless system the minima in the radial and azimuthal velocity distributions must be shifted by $\pi/2$ in wave phase (Lin et al. 1969). For $\lambda = 2$ kpc a phase change of $\Delta\chi = \pi/2$ corresponds to a 0.5-kpc displacement across the arm and can undoubtedly be detectable.

Consider the variations in the two components of the mean cloud velocity perpendicular (U_{\perp}) and parallel (U_{\parallel}) to the shock front with wave phase as obtained by Roberts and Hausman (1984) for models of cloud subsystems with different mean free paths: $p = 0.2$ kpc and $p = 1.0$ kpc (Fig. 2ab). For tightly wound arms, the Galactic radius vector is almost perpendicular to the spiral arms. Therefore, the variation in the mean velocity of a particle ensemble perpendicular to the shock front (U_{\perp}), which is commonly used in gas dynamics, is identical to the variation in the radial residual velocity, implying that $V_R = U_{\perp} + const.$ A similar relation, $V_{\theta} = U_{\parallel} + const.$, also holds for the velocity component U_{\parallel} parallel to the shock front whose variation corresponds to the variation in the azimuthal residual velocity. The wave phase changes in the direction perpendicular to the spiral arm and for tightly wound arms this direction virtually coincides with the direction of the Galactic radius vector. A change in the wave phase χ from 0° to 360° corresponds to an increase in Galactocentric distance R by an amount close to λ .

As we see from a comparison of Figs. 2a and 2b, the profiles of the cloud-velocities variations become more symmetric and the positions of the minima in the radial and azimuthal velocity distributions are shifted from each other with increasing mean free path (i.e., with decreasing importance of collisions). Cloud-cloud collisions cause the asymmetric changes in the profiles of the radial and azimuthal velocities, leading to the coincidence of their minima at the shock front (Roberts and Hausman 1984).

Behind the shock front, where star formation is most intense, the azimuthal velocity varies with Galactocentric distance twice as fast as does the radial velocity (Fig. 2a). Indeed, at the shock front ($\chi = 180^{\circ}$) the two velocity components reach their minima and at the conditional outer arm boundary ($\chi = 270^{\circ}$), the azimuthal component already reaches its maxi-

mum, whereas the radial component increases only to zero (the mean between the peaks in Fig. 2a). Since the abrupt velocity variations with distance are easily blurred by distance errors, the variations in the azimuthal component behind the shock front are more difficult to detect. This may be the reason why we found no statistically significant variations in the azimuthal residual velocity across the Carina arm, although the variations in the radial component across this arm are clearly seen. The variations in the azimuthal velocity across the Carina arm can be simply blurred by distance errors. This removes the serious logical contradiction, because the absence of variations in azimuthal velocity across the Carina arm cannot be explained by any theoretical models.

The fact that we nevertheless see the variations in the azimuthal velocity across the Cygnus and Perseus arms can be explained by their privileged positions. The Perseus arm is located in the outer region of the Galaxy where objects with erroneous distances have strongly different line-of-sight velocities and can be eliminated from the sample. This cannot be done for objects of the Carina arm ($l = 280\text{--}310^\circ$), because the line-of-sight velocity variations with distance in this direction are small. The same difficulty also concerns the Cygnus arm ($l = 75\text{--}100^\circ$), but it is, on average, closer to the Sun than the Perseus and Carina arms, which significantly facilitates its study.

The location of the Corotation Radius

The fact that radial residual velocities of most (70%) of the rich OB associations are directed toward the Galactic center definitely indicates that the region under study is located within the corotation radius (Mel'nik et al. 2001). We consider OB associations with more than 30 stars in the catalog of OB associations by Blaha and Humphreys (1989) to be rich. The model of particle clouds allows us to easily explain the logical relationship between the kinematics of rich OB associations and their location relative to the corotation radius. Let us assume that the star formation in rich OB associations was more intense precisely because of the increase in the frequency of cloud-cloud collisions. The locations of rich OB associations must then coincide with the location of the shock front. And only within the corotation radius the location of the shock front corresponds to the minimum in the cloud radial velocity distribution. Therefore, all of the region under study must be located within the corotation radius or, in other words, the corotation radius in the Galaxy must lie beyond the region under study, i.e., beyond the Perseus arm. This implies that the angular velocity of the spiral

pattern Ω_p must be lower than the mean angular velocity of the Galactic rotation at the Perseus-arm distance. Taking the rotation-curve parameters from Mel'nik et al. (2001), we obtain the following constraint on Ω_p in absolute units: $\Omega_p < 25 \text{ km s}^{-1} \text{ kpc}^{-1}$.

The Mean Free Path of Molecular Clouds and the Axial Ratio of the Velocity Ellipsoid for OB Associations

An analysis of the kinematics of OB associations (Dambis et al. 2001) shows that the axial ratio of the velocity ellipsoid for OB associations in the radial and azimuthal directions is $\sigma_u : \sigma_v = 8.2 : 5.8 = 1.4$. This value is close to the ratio of the amplitudes of the radial and azimuthal velocities for epicyclic motions, $2\Omega/\kappa = 1.6$, where κ is the epicyclic frequency. An axial ratio of the velocity ellipsoid close to the Lindblad ratio $2\Omega/\kappa$ was also obtained for young clusters (Zabolotskikh et al. 2002), implying that the clouds out of which young stars are born move almost freely in epicycles. Therefore, the clouds collide only at the shock front, whereas behind the front and in the interarm space they undergo no collisions and move ballistically. This implies that the cloud mean free path behind the shock front must be larger than the epicycle scale size. For a subsystem with a velocity dispersion of $\Delta u = 6 \text{ km s}^{-1}$ the epicycle radius in an unperturbed region of the Galactic disk is $X \approx 0.2 \text{ kpc}$. Therefore, for a mean free path $p > 0.2 \text{ kpc}$, cloud-cloud collisions will occur mostly at the shock front, which is also confirmed by the direct computations of cloud orbits performed by Hausman and Roberts (1984). Note that local value of a free path depends on cloud density, and its values in the arm and the interarm region can differ by more than a factor of 6 (Levinson and Roberts 1981).

Deviations from an Ideal Spiral Pattern

Figure 3 shows the velocity field of OB associations in projection onto the Galactic plane. The circular arcs in this figure correspond to the minima in the radial (solid line) and azimuthal (dashed line) residual velocity distributions and determine the kinematic positions of the Carina, Cygnus, and Perseus arms. Both deviations from an ideal spiral pattern — the displacement of the Cygnus and Carina arm fragments relative to each other such that they do not form a single, smooth spiral arm and the absence of the Perseus arm extension in quadrant III — are clearly seen in Fig. 3. The extension of the Perseus arm in quadrant III shows up neither in kinematics nor in an increase in the density of young stars.

The kinematic position of the Carina arm ($R = 6.5 \pm 0.1$ kpc) is displaced relative to the Cygnus arm ($R = 6.8 \pm 0.1$ kpc) by 0.3 kpc. This displacement was obtained for the model of ring arms. Its statistical significance is 2σ . The displacement increases to 0.5 kpc for the model of trailing spiral arms even with a small pitch angle, $i = 5^\circ$. Its statistical significance also increases. In contrast, the displacement decreases for the model of leading arms. The problem is that a trailing arm cannot be drawn through the complexes of young objects in Carina and Cygnus, but these complexes fall nicely on a leading arm (Fig. 3).

Spiral Arms and Spurs

The main puzzle of the Galactic spiral structure in the solar neighborhood lies in appreciable nonrandom deviations from an ideal spiral pattern. The images of other galaxies often show deviations from a smooth spiral pattern on short- and intermediate scales, which are usually called spurs. The element of chaos introduced by spurs into the spiral structure of galaxies can also be used, in principle, to explain the defects in the Galactic spiral pattern. Let us use the definition of a spur given by Roberts and Hausman (1984) as a region of intense star formation located far from the line of minimum potential and consider various spur generation mechanisms.

Roberts and Hausman (1984) showed that the possible long delay of star formation behind the shock front leads to a blurring of the spiral arms identified by a concentration of young stars and to the appearance of spurs. The successive star formation in the Galaxy produced by supernova explosions (Gerola and Seiden 1978), also facilitates the formation of spurs. However, in the presence of a density wave the cloud velocity field has a characteristic periodic structure and neither the successive formation nor the delay of star formation has virtually no effect on this field (Roberts and Hausman 1984). Moreover, they facilitate the detection of the periodic cloud velocity-field structure by revealing the cloud velocities and distances at different spiral-wave phases. The fragments of the Carina, Cygnus, and Perseus arms that we identified cannot be spurs of this type, by any means. A comparison of their kinematics with the computed velocity field (Roberts and Hausman 1984) clearly indicates that they are located near the line of minimum potential. The complex of young objects in Sagittarius whose kinematics or, more specifically, the radial residual velocity of young stars directed away from the Galactic center (Fig. 3) is suggestive of its interarm location must be called a spur by the definition of Roberts and Hausman.

Roberts and Stewart (1987) found another spur generation mechanism. They showed that for a large mean free path, individual fragments of the spiral pattern can temporarily shift in phase from each other, while the global spiral pattern of the cloud subsystem can exhibit ruggedness and gaps. The shift of the cloud density maximum (collective sloshing) relative to the potential minimum is produced by the tuning of epicyclic motions of individual clouds (Roberts and Stewart 1987). For collisionless models the displacement of individual arm fragments relative to each other can reach 20% of the interarm distance, while for a system with a mean free path of $p = 0.2$ kpc it does not exceed 5%. However, the collective sloshing mechanism can no longer explain the 0.5 – kpc displacement of the kinematic positions of the Carina and Cygnus arm fragments. The Galactic cloud system is undoubtedly collisional and, consequently, this mechanism cannot produce large deviations from a smooth spiral pattern.

Weaver (1970) found another type of spurs similar to the branches at the outer arm edges. Elmegreen (1980) found their mean pitch angle to be $60^\circ \pm 10^\circ$. Weaver (1970) and Elmegreen (1980) believe that the Orion region is such a spur in our Galaxy. Strong gas compression in the spiral arm, which can trigger the growth of perturbations in a direction almost perpendicular to the arm, can be responsible for the appearance of such spurs (Balbus 1988; Kim and Ostriker 2002). However, the Carina, Cygnus, and Perseus arm fragments that we identified do not belong to this type of spurs either. First, no other spiral arms from which these fragments could appear as spurs are observed. Second, the Cygnus and Perseus arm fragments are definitely elongated in the azimuthal direction (Fig. 3).

Yet another type of spurs in the interarm space was found by Contopoulos and Grosbell (1986, 1988) when studying the nonlinear effects in high-order resonances between the epicyclic frequency and the relative rotation rate of the spiral pattern. The spurs and gaps in the spiral structure near corotation are produced by nonlinear effects, which lead to difference in the shapes and orientations of the periodic orbits inside and outside the $4/1$ resonance ($\kappa/(\Omega - \Omega_p) = 4/1$). The orbits outside the $4/1$ resonance can be oriented in such a way that the maximum of their crowding may not coincide with the spiral arm. However, nonlinear effects arise in the case of high potential perturbation amplitudes and must be observed in galaxies with large arm pitch angles, $i > 30^\circ$ (Contopoulos and Grossbell 1986). The tightly wound spiral pattern of our Galaxy ($i = 5^\circ$) cannot, in principle, undergo nonlinear effects near corotation.

Thus, none of the spur types listed above can explain the peculiar features

of the Galactic spiral structure, more specifically, the deviations from an ideal spiral pattern. The potential perturbation itself is, probably, not an ideal monochromatic spiral wave.

Some authors (Byrd 1983; Byrd et al. 1984) consider the spurs produced by the gravitation of a massive complex rotating in the Galactic disk (gravitational spurs). However, such spurs differ from the spiral-arm fragments only in their length and perturbation amplitude. Both are produced by a gravitational potential perturbation and are located near the potential minimum.

Conclusions

Some of the peculiar features of the periodic velocity-field structure for OB associations (Mel'nik et al. 2001) can be explained by using the model of Roberts and Hausman (1984), in which the behavior of a system of dense clouds is considered in a perturbed potential. The absence of statistically significant variations in the azimuthal velocity across the Carina arm, probably, results from its sharp increase behind the shock front, which is easily blurred by distance errors. The existence of a shock wave in spiral arms and, at the same time, the virtually free motion of OB associations in epicycles can be reconciled in the model of particle clouds with a mean free path of 0.2–2 kpc. The velocity field of OB associations exhibits two appreciable nonrandom deviations from an ideal spiral pattern: a 0.5-kpc displacement of the Cygnus- and Carina-arm fragments from one another and a weakening of the Perseus arm in quadrant III. Nevertheless, the identified fragments of the Carina, Cygnus, and Perseus arms do not belong to any of the known types of spurs. The perturbation of the Galactic potential is, probably, not a monochromatic spiral wave.

The spiral arms of the Galaxy are often compared with those of the Andromeda galaxy. Both galaxies have a tightly wound spiral pattern and similar streaming motions. The mean interarm distance of $\lambda = 3$ kpc observed in the Andromeda galaxy at distances $R = 6$ –16 kpc corresponds to a mean pitch angle of $i = 7^\circ$ (Arp 1964; Braun 1991). The spiral pattern of the Galaxy in the solar neighborhood has similar parameters, $\lambda = 2$ kpc and $i = 5^\circ$ (Mel'nik et al. 1999, 2001). The change in the velocity of neutral and molecular hydrogen clouds across the spiral arms in the Andromeda galaxy is 10–20 km/s (Braun 1991; Neininger et al. 2001), which is close to the velocity of streaming motions of young stars in our Galaxy. In addition, the distribution of HII regions in the Andromeda galaxy also exhibits

deviations of individual arm fragments from an ideal monochromatic spiral pattern (Considerere and Athanassoula 1982; Braun 1991).

Acknowledgments

I am grateful to A.V.Zasov for a discussion and helpful remarks, which contributed to a substantial improvement of the paper. I wish to thank I.I.Pasha, A.S.Rastorguev, and Yu.N.Efremov for useful advice and remarks. The work was supported by the Russian Foundation for Basic Research (projects nos. 02-02-16667 and 00-02-17804), the Council for the Program of Support of Leading Scientific Schools (grant no. 00-15-96627), and Federal Research and Technology Program "Astronomy" .

References

- Adler D.S., and Roberts W.W., *Astrophys. J.* **384**, 95 (1992).
Arp H., *Astrophys. J.* **139**, 1045 (1964).
Balbus S.A., *Astrophys. J.* **324**, 60 (1988).
Blaha C., and Humphreys R.M., *Astron. J.* **98**, 1598 (1989).
Braun R., *Astrophys. J.* **372**, 54 (1991).
Byrd G.G., *Astrophys. J.* **264**, 464 (1983).
Byrd G.G., Smith B.F., and Miller R.H., *Astrophys. J.* **286**, 62 (1984).
Considerere S., and Athanassoula E., *Astron. Astrophys.* **111**, 28 (1982).
Contopoulos G., and Grosbol P., *Astron. Astrophys.* **155**, 11 (1986).
Contopoulos G., and Grosbol P., *Astron. Astrophys.* **197**, 83 (1988).
Dambis A.K., Mel'nik A.M., and Rastorguev A.S., *Astron. Letters*, **21**, 291 (1995).
Dambis A.K., Mel'nik A.M., and Rastorguev A.S., *Astron. Letters*, **27**, 58 (2001). [ftp://lnfm1.sai.msu.ru/pub/PEOPLE/rastor/Dambis et al-2001-OB associations \(eng\).pdf](ftp://lnfm1.sai.msu.ru/pub/PEOPLE/rastor/Dambis%20et%20al-2001-OB%20associations%20(eng).pdf)
Elmegreen D.M., *Astrophys. J.* **242**, 528 (1980).
Gerola H., and Seiden P.E., *Astrophys. J.* **223**, 129 (1978).
Glushkova E.V., Dambis A.K., Mel'nik A.M., and Rastorguev A.S., *Astron. Astrophys.* **329**, 514 (1998).
Hausman M.A., and Roberts W.W., *Astrophys. J.* **282**, 106 (1984).
Kim W.-T., and Ostriker E.C., *Astrophys. J.* **570**, 132 (2002).
Kwan J., and Valdes F., *Astrophys. J.* **315**, 92 (1987).
Levinson F.H., and Roberts W.W., *Astrophys. J.* **245**, 465 (1981).
Lin C.C., Yuan C., and Shu F.H., *Astrophys. J.* **155**, 721 (1969).

Mel'nik A.M., Dambis A.K., and Rastorguev A.S., *Astron. Letters*, **25**, 518 (1999).

Mel'nik A.M., Dambis A.K., and Rastorguev A.S., *Astron. Letters*, **27**, 521 (2001). [ftp://lnfm1.sai.msu.ru/pub/PEOPLE/rastor/Melnik et al-2001-Periodic pattern of OB-associations.pdf](ftp://lnfm1.sai.msu.ru/pub/PEOPLE/rastor/Melnik%20et%20al-2001-Periodic%20pattern%20of%20OB-associations.pdf)

Neininger N., Nieten Ch., Guelin M. et al., *Proceedings of the 205th Symp. of the IAU Galaxies and Their Constituents at the Highest Angular Resolutions*, Ed. by R.T.Schilizzi, S.Vogel et al., (PASP, San Francisco, 2001), p. 352.

Pringle J.E., Allen R.J., and Lubow S.H., *MNRAS* **327**, 663 (2001).

Rastorguev A.S., Pavlovskaya E.D., Durlevich O.V., Filippova A.A., *Astron. Letters*, **20**, 591 (1994).

Roberts W.W., *Astrophys. J.* **158**, 123 (1969).

Roberts W.W., and Hausman M.A., *Astrophys. J.* **277**, 744 (1984).

Roberts W.W., and Stewart G.R., *Astrophys. J.* **314**, 10 (1987).

Solomon P.M., Sanders D.B., and Rivolo A.R., *Astrophys. J. Lett.* **292**, L19 (1985).

Weaver H., in *Interstellar Gas Dynamics*, ed. Habing H., (Dordrecht: Reidel), IAU Symp. **39**, 22 (1970).

Zabolotskikh M.V, Rastorguev A.S., Dambis A.K., *Astron. Letters*, **28**, 454 (2002). <ftp://ftp.sai.msu.ru/pub/groups/cluster/rastor/AL454.pdf>

see my Homepage at <http://lnfm1.sai.msu.ru/~anna>

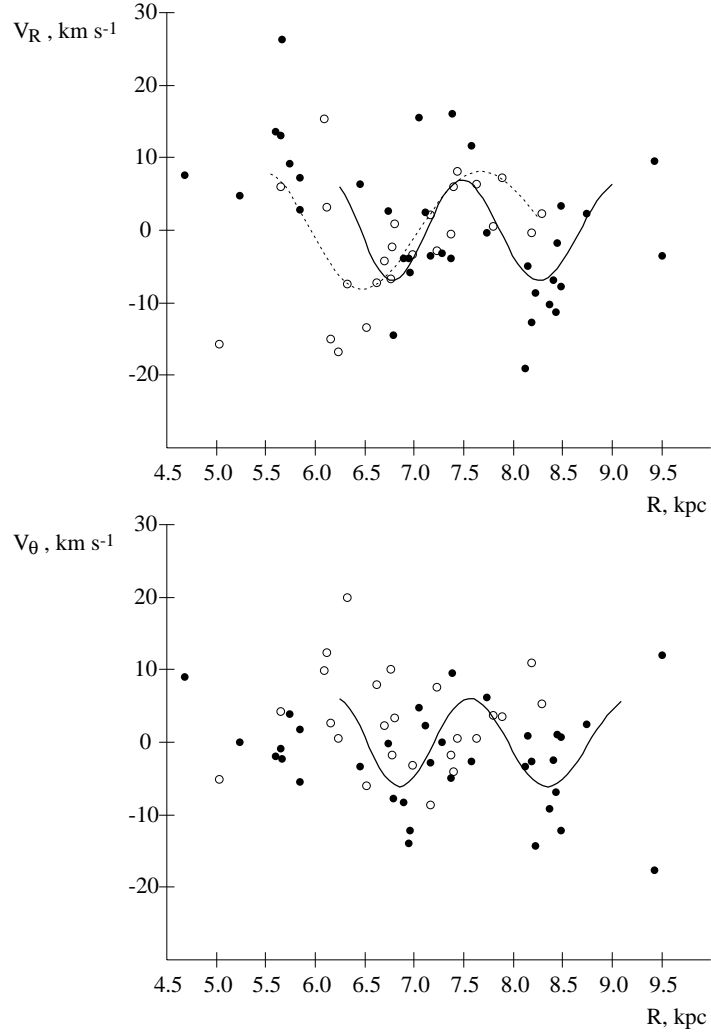


Figure 1: The distribution of the (a) radial (V_R) and (b) azimuthal (V_θ) residual velocities of OB-associations in Galactocentric distance R . OB associations located in the regions $0 < l < 180^\circ$ and $180 < l < 360^\circ$ are represented by filled and open circles, respectively. The sine-wave parameters were determined by solving the equations for line-of-sight velocities and proper-motions in two regions $30 < l < 180^\circ$ (solid line) and $180 < l < 360^\circ$ (dotted line)

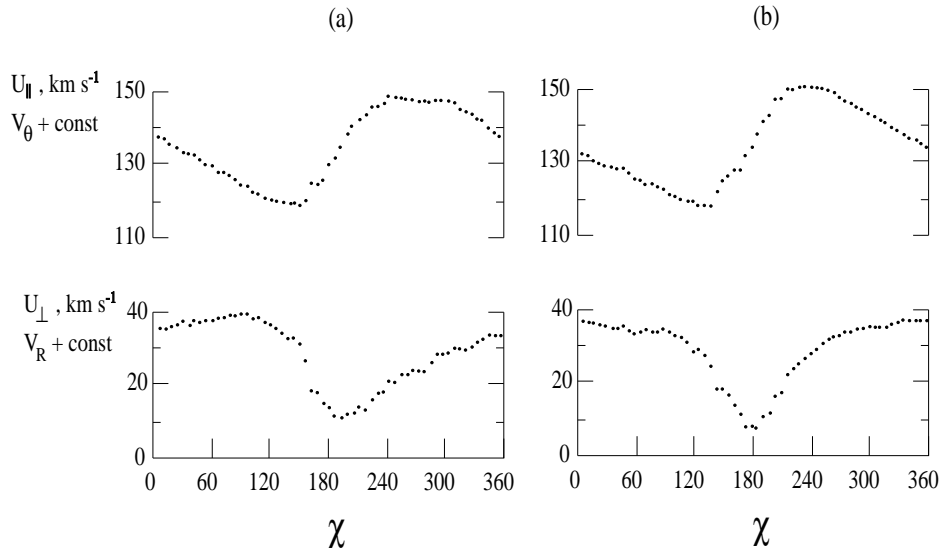


Figure 2: Variations in the cloud velocity components perpendicular (U_{\perp}) and parallel (U_{\parallel}) to the shock front with the spiral-wave phase χ for cloud systems with a mean free path of (a) $p = 0.2$ kpc and (b) $p = 1.0$ kpc (Roberts and Hausman 1984, Fig. 13).

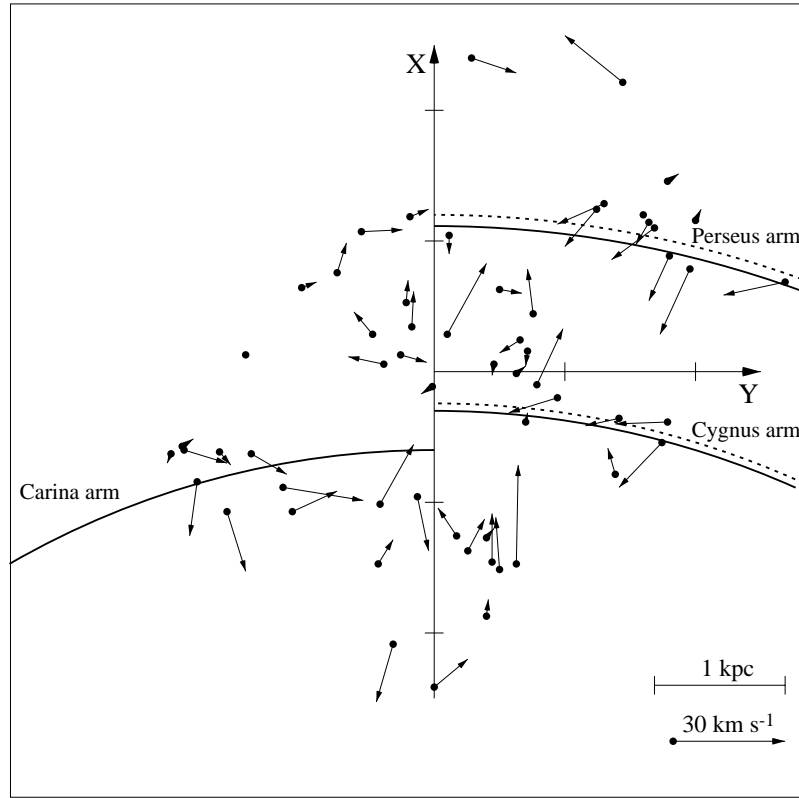


Figure 3: The residual-velocity field for OB-associations in projection onto the Galactic plane. The X axis is directed away from the Galactic center and Y axis is in the direction of Galactic rotation. The Sun is at the coordinate origin. The circular arcs correspond to the minimum radial (solid line) and azimuthal (dashed line) residual velocities of OB associations and determine the kinematic positions of the Carina, Cygnus, and Perseus arms.